are attached to the plate by means of bolts and springs. The cross members q_1, q_2, and the upstream cross members are clamped to the pivot arm, and b_1 is clamped to the test section plate whereas b_2 is fixed directly to the test section plate. The cross-members downstream of q_2 are not attached to the pivot arm. The result is the following. The nozzle contour between P and q_1 and from b_2 on is practically a straight line. The nozzle plate is slightly lifted at q_2 and b_1. The springs are so designed that the displacements at q_2 and b_1 result in local slopes equal to the theoretically desired values. The resulting curvature of the plate, shown by the dashed line in Fig. 2b, is not discontinuous.

The location of b_1 and b_2 is chosen once and for all. For a given Mach number in the test section, the position of q_1 in q_2 has to be such that the characteristics intersect b_1 and b_2 (Fig. 2a). The contour between q_1 and q_2 deviates from the theoretical one and also from the flow between the two characteristics, thus creating a disturbance zone. By means of an analogous deviation between b_1 and b_2, this disturbance is practically completely cancelled so that it is not propagated into the test section.

A suitable system of q cross members is obtained by starting with the highest Mach number and determining the position of q_1 and q_2 for that Mach number. The next lower design Mach number has to be such that the location of the new q_1 coincides with the previous q_2. The new q_2 is then also determined. Proceeding in this manner provides a series of design Mach numbers. The size of the intervals ΔM depends on the distance between b_1 and b_2.

The required displacement Δy is different for each q_2 cross member, but it has an unambiguous value. However at b_1 the value of Δy is a function of Mach number, which can be approximated by a proper choice of the spring constant.

This completes the discussion of the refinements of the aerodynamic design of the nozzle.

The calculation of the curved part of the nozzle was carried out for each Mach number by means of the exact flow equations. Boundary-layer displacement effects are taken into account. The five hydraulic jacks are attached to the cross members, so the jacks are inactive when the associated cross member is clamped to the pivot arm (Fig. 2a). With the remaining active jacks the desired contour can be approximated very well over the complete Mach number range.

3 Concluding remarks

The main design aspects of a flexible nozzle for supersonic wind tunnels were discussed. The discussion centered around the SST design for the CSST minor modifications were introduced for $M > 4$.

The intervals between design Mach numbers are $0.1 < \Delta M < 0.4$ and good flow quality is obtained at intermediate Mach numbers. By means of calibrations, small corrections of the jack extensions can be applied and it appears possible to obtain parallel flow within $|\delta M| < 0.0015M$. The correction per jack is obtained by means of a specially developed but generally applicable optimization method.[3] The method determines the contour corrections from the measured Mach number distribution and also gives the actual flow angularity.

References

[1] Erdmann, S. F., "Design Considerations of the Supersonic Wind Tunnels at NLR," DH 68-04a, Oct. 1968, National Aerospace Laboratory (NLR), Amsterdam, Holland.

[2] Rosén, J., "The Design and Calibration of a Variable Mach Number Nozzle," *Journal of Aeronautical Sciences*, Vol. 22, No. 7, July 1955, pp. 484–490.

[3] Erdmann, S. F., "Optimierung der Düsenform und Bestimmung der lokalen Strömungsrichtung mittels gemessener Geschwindigkeitsverteilungen im Ueberschall," *Zeitschrift für Flugwiss*, 15, Heft 8/9, Aug./Sept. 1967, pp. 305–311.

Trajectories of Particles Suspended in Fluid Flow Through Cascades

W. Tabakoff* and M. F. Hussein†
University of Cincinnati, Cincinnati, Ohio

Introduction

THE study of the trajectories and velocities of solid particles suspended in a fluid flow passing through a cascade nozzle is of importance to the investigation of erosion damage sustained by the blades. In general, the trajectories and velocities of the particles depend upon the slope of the cascade nozzle, particle and flow inlet conditions, particle material density, mean diameter, angle of attack and initial place of collision. The particles are more likely to follow the fluid streamlines when their material density is of the same order of magnitude as that of the fluid and when their mean diameter is small.

In this experimental investigation, a cascade row of turbine blades was mounted in a cascade tunnel to produce the desired gas-particle flow. A high-speed camera was used to photograph the flow. The film analysis provided the data for the particle velocities and the particle paths through the cascade nozzle.

Test Facilities and Conditions

A special subsonic cascade wind tunnel, designed for gas-particle studies, was used for this series of tests. Reference 1 gives a detailed description of the tunnel and the airfoil used in the cascade nozzle.

A high speed motion picture camera with a maximum speed of 6000 frames-sec at 220-v input was used to photograph the particulate flow. Solid particles of 1000-μ mean diameter and 1.1-g/cm^3 density were used. The range of particle diameters available was limited by the fact that if particles of smaller diameters were used, it was impossible to determine their trajectories from a film analysis. A direct lighting technique was used in the experiments, and the

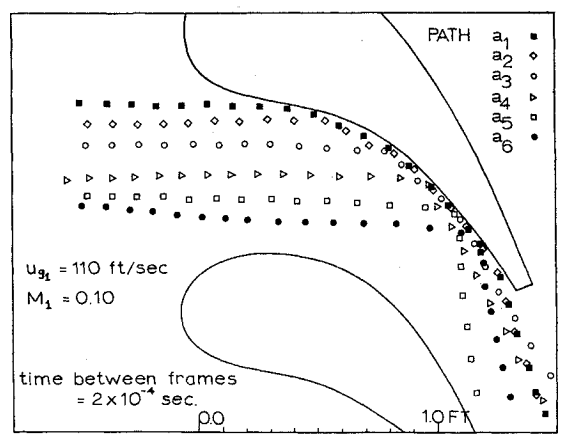

Fig. 1 Trajectories of particles entrained by gas flow (path a).

Presented as Paper 70-712 at the AIAA 6th Propulsion Joint Specialist Conference, San Diego, Calif., June 15–19, 1970; submitted July 13, 1970. This work was sponsored under Project Themis Contract Number DAHCO 4-69C-0016, U.S. Army Research Office—Durham.

* Professor, Department of Aerospace Engineering. Associate Fellow AIAA.

† Graduate Research Assistant, Department of Aerospace Engineering. Student Member AIAA.

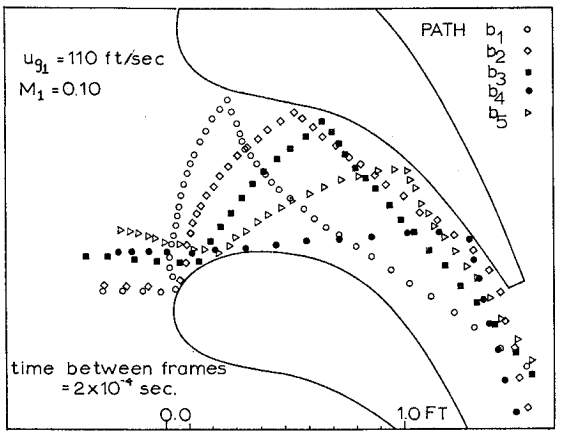

Fig. 2 Trajectories of particles entrained by gas flow (path b).

background was varied appropriately to the color of the particles to give maximum contrast and clearness of photograph.

The camera and lights were mounted on special stands to provide fine focusing and to minimize any vibrations during the run. An electronic timer was used to obtain film markings at intervals of 0.001 sec. These markings were then used to estimate an accurate film speed. The distance traveled by a particle was calculated from observation of its location on two successive frames. The particle velocity at a point could then be determined since the time between two frames was known.

The particles were injected at a calibrated concentration using the particle injector of Ref. 2.

The camera speed was set at 6000 frames/sec and lighting intensity at 200,000 ft-c. Film rolls of 400 ft were used, and the camera reached its maximum speed after the first 100 ft of the film. The run time was approximately 3 sec.

Test Results and Discussion

From the analysis of the film, the trajectories of particles can be classified in three main groups (see Figs. 1–3). It can be seen from Fig. 1 that the majority of particles enters the cascade nozzle without colliding with the leading edge, and subsequently impinge on the blade pressure side. The particles then rebound and leave the nozzle. The possibility of a particle impinging again on the suction side near the rear, e.g., path a_5, depends on its initial collision location and angle of attack. Figure 2 shows that some of the particles hit the upper part near the leading edge of the blade and then, before leaving the nozzle with the outlet flow, travel laterally until

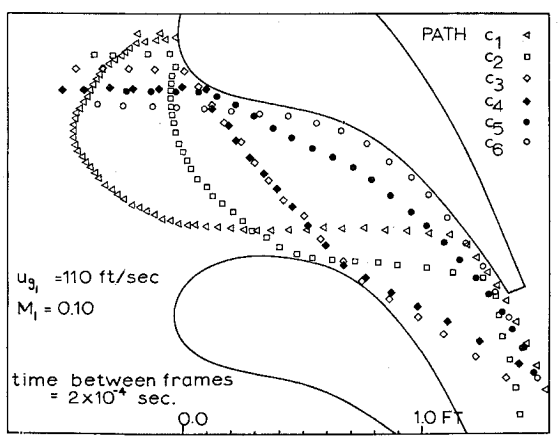

Fig. 3 Trajectories of particles entrained by gas flow (path c).

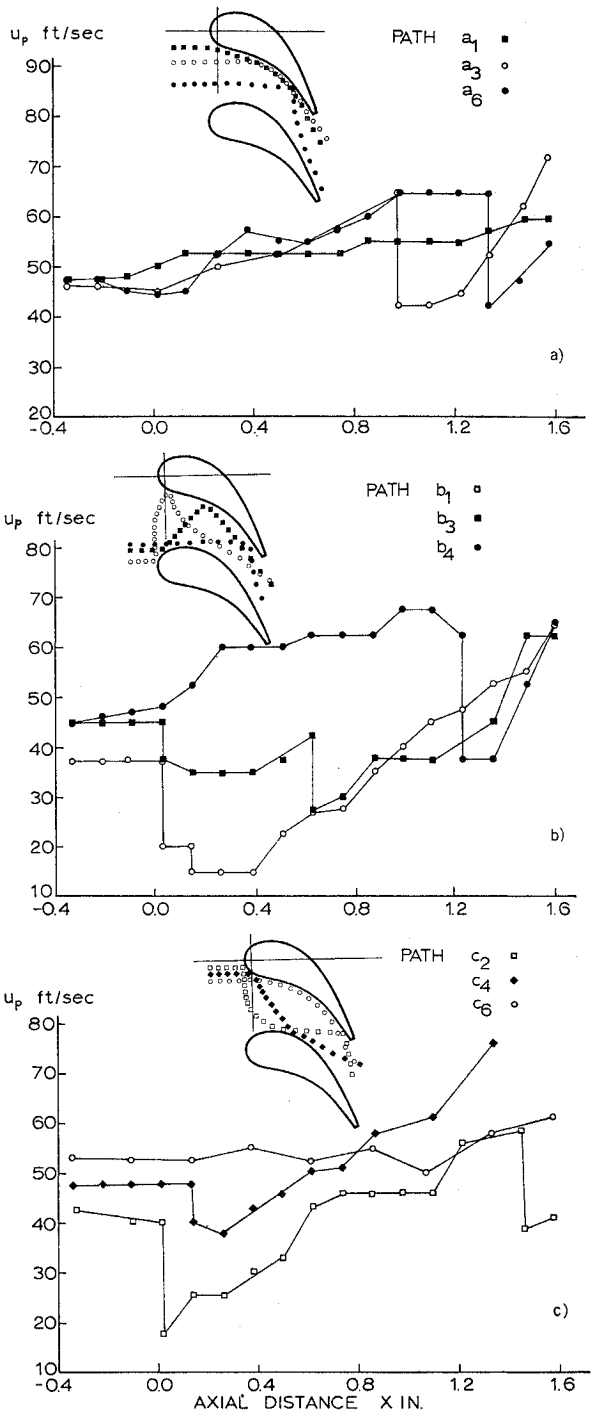

Fig. 4 Velocity of particles entrained by gas flow.

rebounding from the pressure side. The place of collision with blade pressure side depends on the particle incidence and its initial impact location. In path b_1 particles hit the pressure side near the leading edge, while in path b_4, they hit it at the rear. Some of the particles may have the tendency to hit the blade suction side at the rear after colliding with the pressure side as in path b_4. Figure 3 shows that some particles impinge on the lower part near the leading edge of the blade, rebound, and then sometimes, depending on their initial velocity and place of collision, collide with blade suction side (i.e., see paths c_1, c_2, c_3, c_4, c_5, and c_6).

Finally, there are those particles which cannot be classified following the above scheme; however, they are few in number and consequently can be neglected.

To obtain the previous results, the inlet gas velocity was set

at $u_{q1} = 110$ fps, the inlet Mach number at $M_1 = 0.1$ and the particle concentration (α) at 0.02.

The concentration factor α is defined as the ratio of mass flow rate of particles to the total mass flow rate of the gas and particles mixture, or

$$\alpha = W_p/(W_p + W_g)$$

where W_p = rate mass flow of particles, lb/sec and W_g = rate of air mass flow, lb/sec.

Numerous tests have been performed for different inlet conditions, but only one of these test runs are shown in the figures.

The velocity profiles for some of the solid particle paths in Figs. 1–3 are shown in Fig. 4, parts a), b), and c), respectively. Figure 4a shows the solid-particle velocity profiles for paths a_1, a_3, and a_6. The inlet particle velocity u_{p_1} is approximately constant 0.4 of the inlet gas velocity. Figure 4b presents the solid-particle velocity profiles for paths b_1, b_3, and b_4. Figure 4c gives the velocity of the solid particles for paths c_2, c_4, and c_6. It can be seen from Fig. 4 that the solid particle velocities are always lagging the gas flow velocity as predicted in Ref. 2.

Also, it was observed that the particles with increasing diameter and relatively large density tend not to follow the fluid stream lines. Trajectory computations also show that the blade leading edge and rear parts of the suction and pressure sides are the most likely places for severe blade erosion. An increase in the flow inlet Mach number will cause these trajectories to stretch in the axial direction, but no significant change in the general trends was observed.

A similar study with the same cascades was performed using a water table. Results show that the solid particles follow the water stream lines approximately, and collisions with the blade boundary were observed only at the blade leading edges. Particle velocities continue to increase as the particle goes through the cascade nozzle but always lag behind the water speed.

Conclusions

For incompressible flow, it is evident that the particle trajectory can easily be predicted since, as shown with the water table, the solid particles follow the flow streamlines. On the other hand, for compressible flow, wind tunnel experiments indicate that the particle trajectories are very difficult to predict analytically, especially if the size of the solid particles is over 50μ.

References

[1] Tabakoff, W. and Hussein, M. F., "An Experimental Study of the Effect of Solid Particles on the Pressure at Blade Surfaces in Cascade," Project Themis Report 70–8, March 1970, Univ. of Cincinnati; also Rept. AD-703896, U.S. Government Research and Development.

[2] Tabakoff, W. and Hussein, M. F., "Properties and Particle Trajectories for Gas-Particle Flows in Cascades," AIAA Paper 70-712, San Diego, Calif., 1970.